Correlation imaging reveals specific crowding dynamics of kinesin motor proteins

Miedema, D.M.; Kushwaha, V.S.; Denisov, D.V.; Acar, S.; Nienhuis, B.; Peterman, E.J.G.; Schall, P.

DOI
10.1103/PhysRevX.7.041037

Publication date
2017

Document Version
Other version

Published in
Physical Review X

License
CC BY

Supplementary Materials for

Correlation imaging reveals specific crowding dynamics of kinesin motor proteins

Daniël M. Miedema, Vandana S. Kushwaha, Dmitry V. Denisov, Seyda Acar, Bernard Nienhuis, Erwin J.G. Peterman, Peter Schall

This document includes:

Supplementary Figures 1-7
Supplementary Tables 1-4

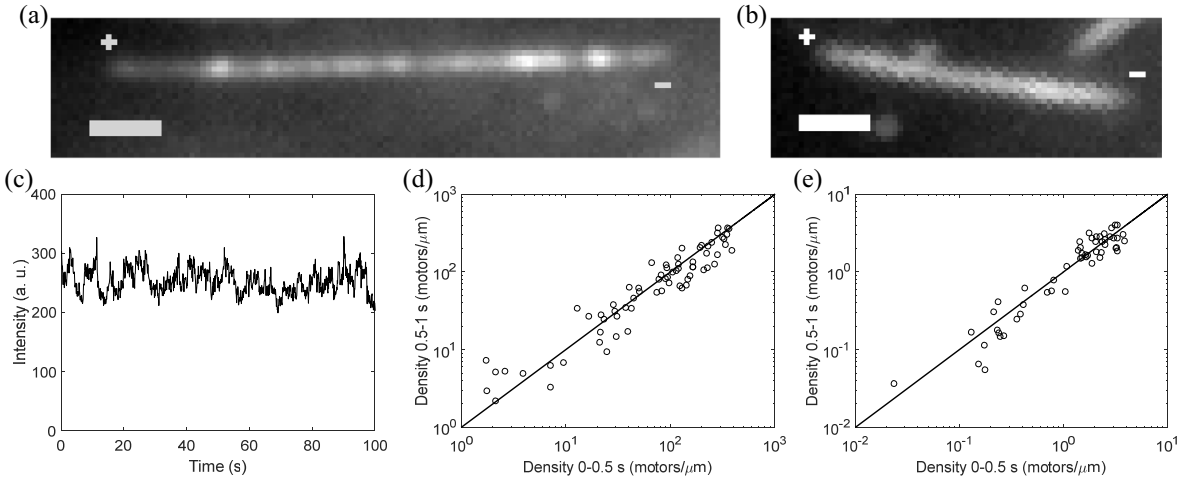

Supplementary Figure 1. Steady-state crowding measurements in the bulk of microtubules. (a,b) Intensity profiles of time averaged TIRF images taken at high motor densities. The homogeneity of motors along microtubules demonstrates that crowding is not restricted to the plus end, but occurs in the bulk of microtubules. (a) 200 nM Kinesin-1 motors of which 20 nM fluorescently labeled in PEM80 buffer. (b) 800 nM OSM-3 motors of which 40 nM fluorescently labeled in PEM80 buffer. The plus and minus ends of the microtubules are indicated. Scale bar is 1 micrometer. (c) Time series of the spatially averaged intensity from fluorescently labeled Kinesin-1 motors. (d,e) Density calculated from the first half of a time-lapse, versus the density calculated during the second half of the time-lapse for OSM-3 (d) and Kinesin-1 (e). Total duration of time-lapses are 50 s for OSM-3 and 100 s for Kinesin-1. Each dot represents density measurements from individual microtubules.

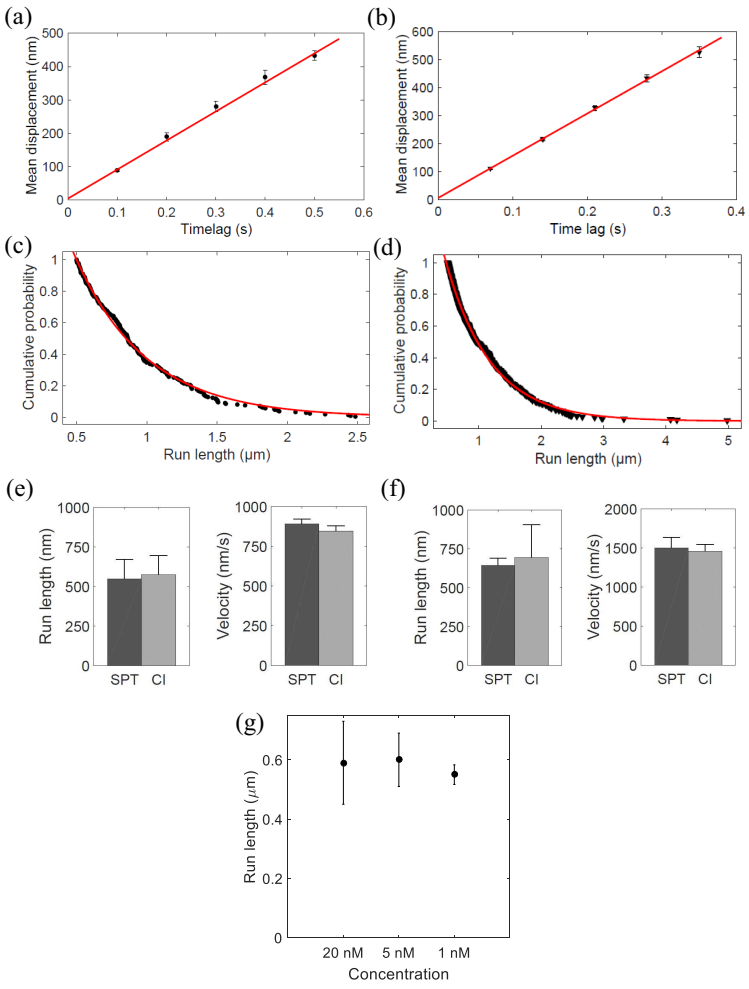

Supplementary Figure 2. Single particle tracking compared to correlation imaging. (a-d) Single particle tracking method to obtain velocity (a,b) and run length (c,d). (a,b) Mean displacement derived from Gaussian fits to mean-displacement histograms versus time lag for Kinesin-1 (a) and OSM-3 (b). The slope of the red linear fit yields the average motor velocity. (c,d) Exponential fit (red line) to cumulative run length distribution yields the average run length for Kinesin-1 (c) and OSM-3 (d). (e,f) Comparison of single particle tracking (SPT) results to correlation imaging (CI) results for 20 nM Kinesin-1 (e) and 40 nM OSM-3 (f) in PEM80 buffer. Both methods are applied to the same 6 microtubules for each condition. (g) Run length of Kinesin-1 motor proteins. The concentration of fluorescent motors varies as indicated, while the total concentration is 20 nM in all experiments. Error bars show the standard deviation.

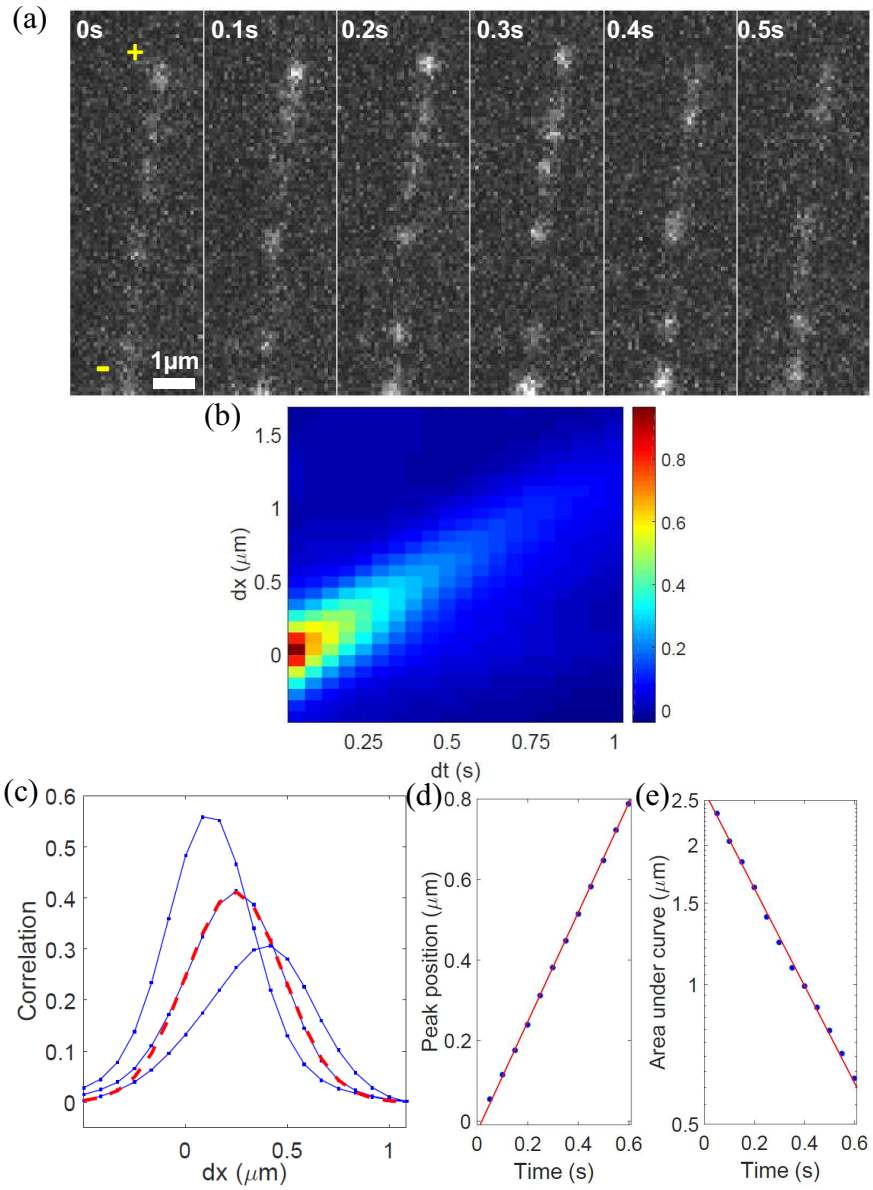

Supplementary Figure 3. Correlation imaging at single particle tracking densities. (a) Time series of fluorescently labeled OSM-3 motor proteins on a microtubule at a concentration of 40 nM in PEM80 buffer. The plus and minus ends of the microtubule are indicated. (b) Spatio-temporal map of correlation of the intensity, of the complete image sequence (1000 images) shown in (a). Values of high correlation lie along a straight line, the slope of which represents the average velocity of the motors. (c) Cross-sections of the correlation surface in (b) at delay times dt=0.1 s, 0.2 s, and 0.3 s. Gaussian fitting (dashed red line) is used to obtain the peak position and area under these curves. (d) Peak position as a function of time. The red linear fit yields the motor velocity. (e) Area under the curve as a function of time in semi-logarithmic representation. The red exponential fit yields the detachment rate of motors.

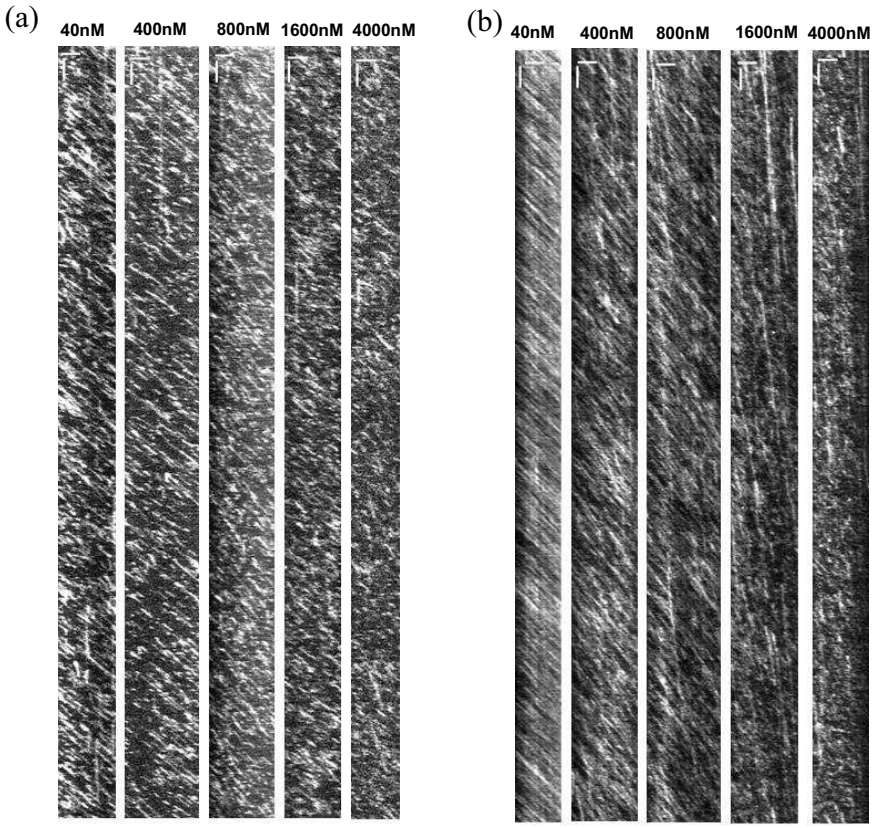

Supplementary Figure 4. Kymographs with a constant concentration of fluorescently labeled OSM-3 motors. Kymographs (time-space plots; scale bars: 2 μm (horizontal) and 2 s (vertical)) of motility assays of OSM-3 motor proteins in PEM80 (a) and PEM12 (b) buffers. The fluorescently labeled OSM-3 concentration is 40 nM in all experiments, the total OSM-3 concentration is indicated above the kymographs.

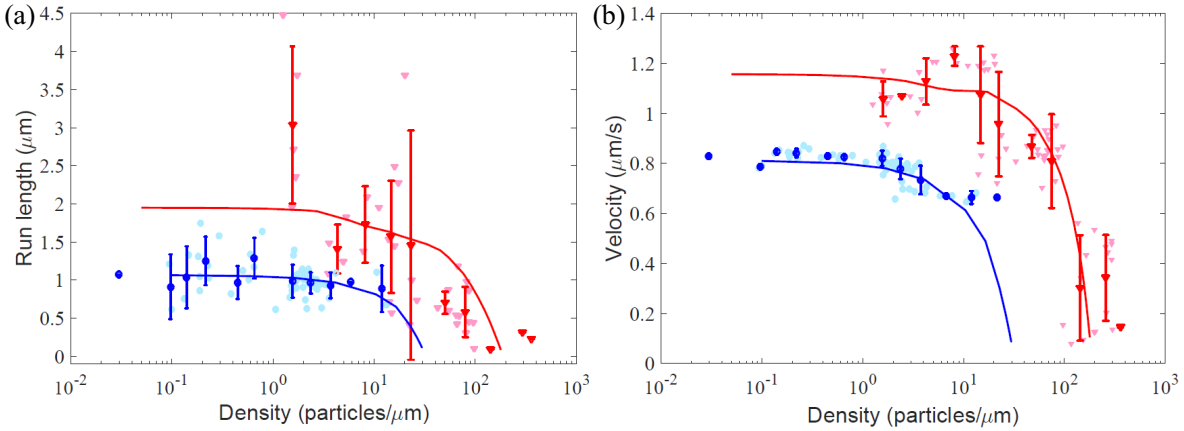

Supplementary Figure 5. Run length increases at lower ionic buffer strength. Experimental data and simulations with the extended TASEP-LK model for OSM-3 and Kinesin-1 motors in low ionic strength buffer PEM12. Run length (a) and velocity (b) as a function of density for Kinesin-1 (blue dots) and OSM-3 (red triangles). Solid curves of the corresponding color show predictions of the extended TASEP-LK model. Error bars show the standard deviation. Numerical values of the experimental data used for fitting are listed in Supplementary Table 4.

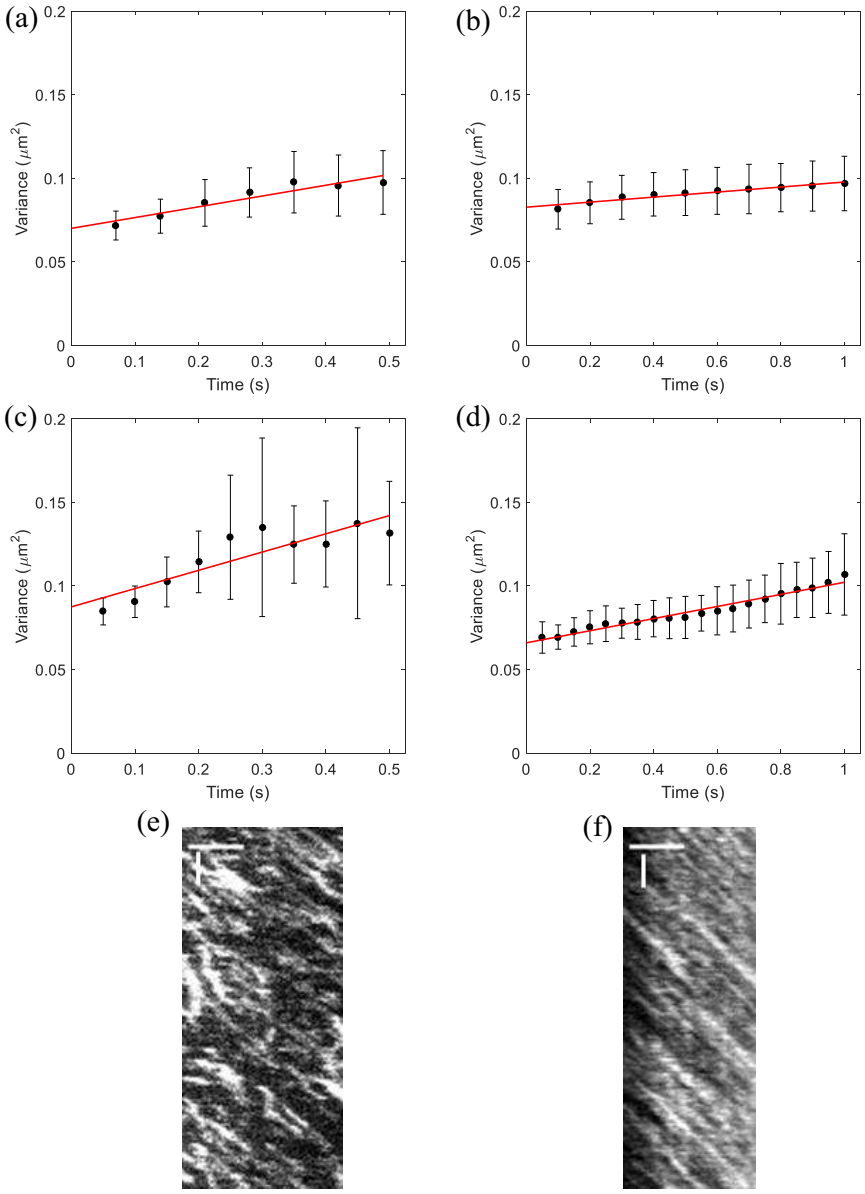

Supplementary Figure 6. Variance of motor velocities increases faster at high ionic strength, indicating more intermittent dynamics. (a-d) Increase in width of the correlation peak over time quantified by the variance of the peak. The linear increase in variance of the correlation peak reflects the increase in variance of motor velocities. Experimental data is shown by black dots with standard deviation error bars and red line indicates best linear fit. (a) 20 nM Kinesin-1 in PEM80, slope 0.07 $\mu m^2/s$. (b) 20 nM Kinesin-1 in PEM12, slope 0.015 $\mu m^2/s$. (c) 40 nM OSM-3 in PEM80, slope 0.1 $\mu m^2/s$. (d) 40 nM OSM-3 in PEM12, slope 0.036 $\mu m^2/s$. (e,f) High-resolution kymographs (time-space plots; scale bars: 2 μm (horizontal) and 2 s (vertical)) of 40 nM OSM-3 motors, showing individual sfGFP-labeled motor trajectories in PEM80 (e) and PEM12 (f) buffer conditions. Individual trajectories in PEM12 are much more straight, less intermittent and appear longer compared to those at PEM80, in line with the smaller increase of the variance in panel (d) compared to panel (c).

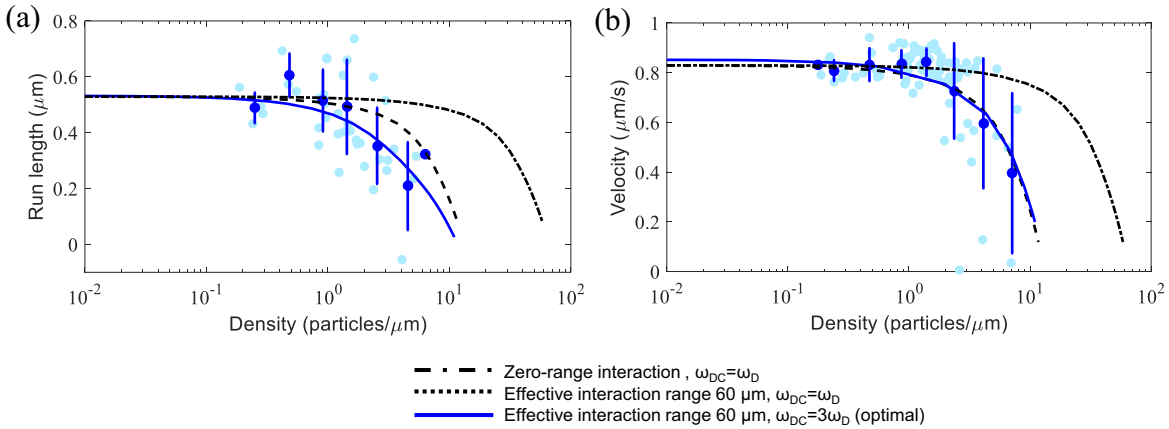

Supplementary Figure 7. The extended TASEP-LK applied to Kinesin-1. Run length (a) and velocity (b) as a function of density. Light blue dots show measurements from single microtubules; dark blue symbols show averages and standard deviations over these measurements within density intervals of logarithmic size. Predictions of the original TASEP-LK model are shown by the dash-dotted black curves. The dotted black curves result from rescaling the density by a factor 5 (effective interaction range 60 nm). The best fit for both run length and velocity is achieved with a detachment rate of constrained motors $\omega_{DC} = 4.5\ \mathrm{s}^{-1}$, shown by the solid blue curve.

	OSM-3 PEM80	Kin-1 PEM80	OSM-3 PEM12	Kin-1 PEM12
motor size, nm	16	16	16	16
motor step, nm	8	8	8	8
affinity ω_{A0} ($\omega_A = \omega_{A0} \cdot c$), μm^3/s	$2.9 \cdot 10^{-5}$	$9.1 \cdot 10^{-5}$	$2.9 \cdot 10^{-5}$	$9.1 \cdot 10^{-5}$
detachment rate ω_D, s^{-1}	2.3	1.55	0.58	0.68
detachment rate constrained motors ω_{DC}, s^{-1}	11.5	4.65	0.58	0.68
step frequency, s^{-1}	175	105	145	105
number of lanes	3	1	3	1
interaction range, nm	0	60	0	15
velocity at $\rho \to 0$, μm/s	1.45	0.85	1.15	0.85
run length at $\rho \to 0$, μm	0.6	0.55	1.95	1.25

Supplementary Table 1. Fitting and derived parameters for the modified TASEP-LK model for motor proteins OSM-3 and Kinesin-1 in buffer solutions PEM80 and PEM12.

OSM-3 PEM80		Kin-1 PEM80	
concentration, nM	density, $1/\mu$m	concentration nM	density, $1/\mu$m
8	0.6±0.46	8	0.32±0.14
40	1.65±0.65	10	0.76±0.37
200	8.78±3.79	20	1.23±0.37
400	14.69±2.4	40	1.7±0.52
800	32.44±15.07	60	2.79±1.21
1600	69.13±17.8	100	2.45±1.18
4000	78.24±42.8	200	4.72±2.73
		400	4.51±2.54
		800	6.71±2.28

Supplementary Table 2. Averaged experimental data of the density-concentration dependence for OSM-3 and Kinesin-1 motors in PEM80 buffer, shown in Fig. 3(c).

OSM-3 PEM80				Kin-1 PEM80			
density, $1/\mu$m	run length, μm	density, $1/\mu$m	velocity, μm/s	density, $1/\mu$m	run length, μm	density, $1/\mu$m	velocity, μm/s
1.36	0.62±0.21	0.08	1.35±0.13	0.25	0.49±0.05	0.18	0.83±0
2.06	0.55±0.07	0.12	1.39±0.18	0.48	0.60±0.08	0.24	0.81±0.04
3.49	0.68±0	0.18	1.30±0.02	0.91	0.51±0.11	0.47	0.83±0.07
5.76	0.42±0.03	1.33	1.33±0.08	1.43	0.49±0.17	0.87	0.83±0.05
13.12	0.47±0.12	2.09	1.32±0.10	2.54	0.35±0.14	1.40	0.84±0.05
20.18	0.40±0.05	3.49	1.43±0	4.54	0.21±0.16	2.36	0.72±0.19
42.85	0.36±0.05	6.68	1.55±0.04	6.36	0.32±0	4.12	0.59±0.26
68.74	0.32±0.06	13.47	1.40±0.12			7.12	0.39±0.32
		20.05	1.38±0.20				
		40.37	1.33±0.13				
		72.66	1.15±0.18				

Supplementary Table 3. Averaged experimental data of the run length and velocity for OSM-3 and Kinesin-1 motors in PEM80 buffer, shown in Fig. 4.

OSM-3 PEM12				Kin-1 PEM12			
density, $1/\mu$m	run length, μm	density, $1/\mu$m	velocity, μm/s	density, $1/\mu$m	run length, μm	density, $1/\mu$m	velocity, μm/s
1.56	3.03±1.03	1.59	1.06±0.07	0.03	1.07±0	0.03	0.83±0
4.34	1.41±0.32	2.44	1.07±0	0.1	0.91±0.42	0.1	0.79±0.01
8.17	1.73±0.5	4.24	1.13±0.09	0.14	1.04±0.41	0.14	0.85±0.01
14.75	1.57±0.74	8.17	1.23±0.04	0.21	1.25±0.32	0.22	0.84±0.02
23.14	1.46±1.5	14.75	1.07±0.19	0.45	0.97±0.22	0.45	0.83±0.01
50.38	0.7±0.15	22.36	0.96±0.21	0.65	1.29±0.27	0.65	0.82±0.01
79.81	0.58±0.33	47.53	0.87±0.05	1.56	0.99±0.22	1.56	0.82±0.03
142.42	0.09±0	74.73	0.81±0.19	2.36	0.96±0.14	2.37	0.78±0.04
292.92	0.31±0	143.17	0.3±0.21	3.71	0.93±0.17	3.74	0.73±0.06
360.11	0.23±0	257.19	0.34±0.17	5.84	0.97±0	6.76	0.67±0
		360.11	0.14±0	11.95	0.89±0.3	11.95	0.66±0.03
						21.44	0.66±0

Supplementary Table 4. Averaged experimental data of the run length and velocity for OSM-3 and Kinesin-1 motors in PEM12 buffer, shown in Supplementary Fig. 5.